Appl. Phys. B 72, 257–261 (2001) / Digital Object Identifier (DOI) 10.1007/s003400000479

Applied Physics B
Lasers
and Optics

Rapid communication

Spatially resolved absolute concentration and fluorescence-lifetime determination of H_2CO in atmospheric-pressure CH_4/air flames

D.I. Shin*, **T. Dreier, J. Wolfrum**

Universität Heidelberg, Physikalisch Chemisches Institut, Im Neuenheimer Feld 253, 69120 Heidelberg, Germany

Received: 25 September 2000/Published online: 30 November 2000 –

Abstract. Using laser-induced fluorescence (LIF), spatially resolved concentration profiles of formaldehyde (H_2CO) were obtained in the preheating zone of atmospheric-pressure premixed CH_4/air flames stabilized on the central slot of a multiple-slot burner similar in construction to domestic boilers. The isolated $pQ_1(6)$ rotational line (339.23 nm) in the $2^1{}_0 4^1{}_0$ vibronic combination transition in the $\tilde{A}^1A_2 - \tilde{X}^1A_1$ electronic band system around 339 nm was excited in the linear LIF intensity regime. For a quantification of quenching effects on the measured LIF signal intensities, relative fluorescence quantum yields were determined from direct fluorescence lifetime as a function of height above the slot exit. Absolute H_2CO number densities in the flames were evaluated from a calibration of measured LIF signal intensities versus those obtained in a low-pressure sample with a known H_2CO vapor pressure. Peak concentrations in the slightly lean and rich flames reached (994 ± 298) and (174 ± 52) ppm, respectively.

PACS: 33.50.Pq;42.62.Fi;82.40.Py

Spatially resolved in situ concentration determination of important intermediate diatomic species in laboratory flames as well as in technical combustion systems is an important task in the critical validation of combustion modeling [1–4]. However, non-intrusive (i.e., optical) diagnostics has been performed much less extensively for polyatomic species. Furthermore, most of these investigations employed sampling probe techniques or absorption methods. For absolute concentration measurements in flames, species-specific data on molecular line strengths, linewidths, quenching efficiencies, etc. are necessary.

Formaldehyde (H_2CO) represents one of few four-atomic species with readily accessible fluorescence states for which well-known spectroscopic information is available [5, 6]. H_2CO is an important intermediate species in the oxidation of hydrocarbons as it is typically formed in cold-flame regions or near the flame front. Recently, Paul et al. [7, 8] pointed out the significance of H_2CO as an indicator for chemical heat release in hydrocarbon-fueled flames. Laser-induced fluorescence (LIF) measurements of native H_2CO in flames have been reported by Harrington and Smyth [9] and earlier by Garland [10]. Planar LIF imaging was performed in engines by Bäuerle et al. [11], and recently in flames by Bombach et al. [12]. However, quantitative concentration measurements proved to be difficult. In contrast to diatomics, the conversion of LIF signal intensities into concentration values is less straightforward for polyatomic species because the temperature dependence of the Boltzmann fraction in the probed ground electronic quantum state can be calculated less precisely due to the dense energy-level structure. In addition, information for the *A*-state of formaldehyde on species-specific collisional quenching at elevated temperatures is limited. Paul et al. [7] presented a theoretical investigation on the temperature dependence of the H_2CO LIF signal intensity and estimated quenching cross sections for typical flame environments. Harrington et al. [9] accounted for the change in partition function with temperature and for effects of collisional quenching in their measurement of relative H_2CO concentration profiles. Until now however, absolute H_2CO concentration determinations were performed only by direct microprobe sampling [13] or spatially integrating absorption techniques [14].

To determine absolute H_2CO concentrations in flames via LIF, overall account can be taken of the local quenching environment – i.e., the relative fluorescence quantum yield – through a measurement of the effective fluorescence lifetime at the spatial position where the measurements have been done. This method has been applied to OH, CH and CN in low-pressure flames [15–17]. At atmospheric pressures and above, the measurement of quenching rates can be done only with picosecond time resolution, a technique which has been applied to OH [18] and CN [19]. However, the effective fluorescence lifetime of the singlet *A*-state of H_2CO even at atmospheric pressure is sufficiently long to make direct calibration feasible using narrowband nanosecond pulses [20].

In the present work we performed spatially resolved measurements of effective fluorescence lifetimes of H_2CO

*Corresponding author.
(Fax: +49/6221-544255, E-mail: dong-ill.shin@urz.uni-heidelberg.de)

for a selected $\tilde{A}^1A_2$-state transition around 339 nm in an atmospheric-pressure premixed CH_4/air flame stabilized on a multiple-slot burner of technical importance. The possible variations of the LIF intensity due to the varying quenching environment with position in the flame were thus corrected by recording the fluorescence decay times for each measurement location. Furthermore, quantitative H_2CO concentration measurements were obtained for two different flame conditions by calibrating the LIF-signal intensities with those from a known amount of formaldehyde enclosed in a low-pressure reference cell at room temperature.

1 Experimental approach

1.1 Burner facility

Measurements of formaldehyde were performed in premixed flames stabilized on the multiple-slot burner shown in Fig. 1, which is described in more detail in [21, 22]. The burner consisted of seven identical slot nozzles (3 mm wide, 150 mm long) for the premixed gases, and secondary air was fed through the 16 mm wide gaps between them. The burner is similar in construction to domestic household boilers. All measurements were performed in the center of the central-slot flame operated simultaneously with all other slots. Table 1 lists the operating parameters for the two flames investigated in this study – a fuel-rich and a slightly lean flame (flames 1 and 2, respectively). The combustion chamber was formed by a 115 mm high flow channel with quartz windows for optical access. The burner was mounted on two translation stages which allowed spatially resolved measurements along a vertical (Y) and horizontal (X) axis with an accuracy of $\pm 100\,\mu$m. To fully characterize the flames, temperature profiles for flames 1 and 2 in the same burner were acquired by other groups within the collaborative project using CARS and fine-wire thermocouples [21].

1.2 LIF experiment and H_2CO *detection*

Laser-induced fluorescence (LIF) measurements were conducted with a tunable dye laser (Lambda Physik, Scanmate) operated with PTP in dioxan and pumped by a XeCl excimer laser (Lambda Physik, EMG 103, 80 mJ/pulse, 10 Hz repetition rate). Typical pulse energies were 3.5 mJ with a bandwidth of $0.25\,\mathrm{cm}^{-1}$. All measurements were performed as a function of height along the vertical axis (Y axis in Fig. 1). The excitation beam was aligned parallel to the flame front (Z axis in Fig. 1).

The experimental setup is described in more detail in [22]. The formaldehyde samples for the calibration measurements were prepared following the method of Spence and Wild [23]. The vapor was contained in a $5 \times 4.5 \times 10$ cm pyrex cell with three UV transparent windows. The cell was filled with (4 ± 0.06) mbar H_2CO vapor and slightly heated from outside during the LIF measurement to avoid adsorption at the cell walls. For concentration and calibration measurements we selected the $2^1_0 4^1_0$ vibronic band of the $\tilde{A}^1A_2 - \tilde{X}^1A_1$ system at 339 nm. Although energy levels in the $2^1_0 4^1_0$ band are known to be dissociative, the large absorption cross section ($5.8 \times 10^{-20}\,\mathrm{cm}^2\,\mathrm{molecule}^{-1}$ at 339.03 nm [24]) compensates the low quantum yield. A spherical lens ($f = 500$ mm) focused the incident laser beam to a diameter of 100 μm to achieve adequate spatial resolution. Fluorescence from all transitions located between 380 and 500 nm was collected behind a stray-light-rejecting long-pass filter (GG 375). Raman signals from the major species CH_4, N_2 and O_2 between 360 and 370 nm are suppressed by the longwave-pass filter and possible interferences were subtracted in measurements on and off resonance of the transition. Fluorescence radiation was detected with a photomultiplier tube whose output voltage was captured with a gated integrator (SRS, mod. SR250). Time-resolved LIF intensities were recorded with a digital storage oscilloscope

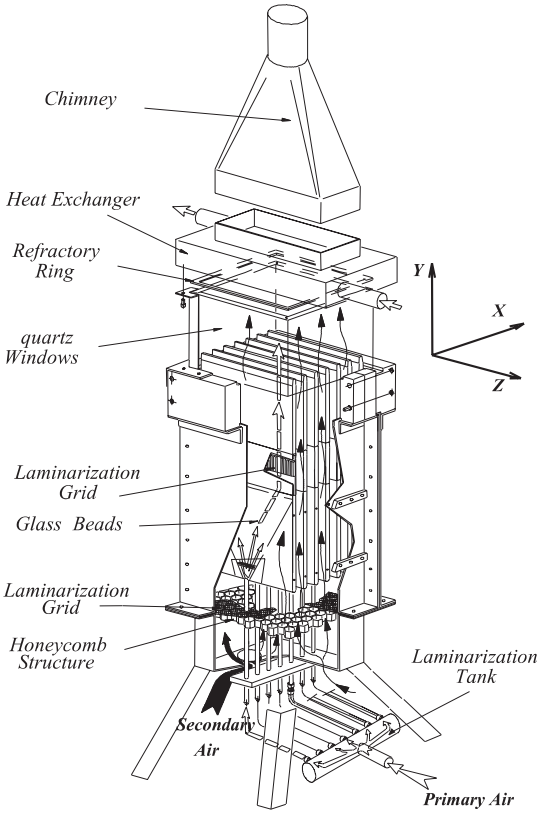

Fig. 1. Schematic of the 7-slot atmospheric-pressure premixed flame burner with heat exchanger and optical access for spatially resolved probing via laser-induced fluorescence (LIF)

Table 1. Operating parameters for the two flame-test case conditions used in the 7-slot burner depicted in Fig. 1. (N) denotes normal cubic meter or liter, respectively; Prim./Second.: primary/secondary; aerat.: aeration

Flame test case	Heating power [kWh/m^3(N)]	Power input [kW]	CH_4gas flow [l(N)/min]	Prim. aerat	Second. aerat	Prim. air flow [l(N)/min]	Second. air flow [l(N)/min]
1	9.97	10	16.7	0.6	0.8	95.5	127.3
2	9.97	10	16.7	1.2	0.2	191	31.8

(LeCroy, 9350 A, 500 MHz bandwidth). From chemical kinetics modeling and quantitative measurements in similar flames, H_2CO is predicted to be produced in comparatively large amounts (> 100 ppm [25]) and thus trapping of the emitted fluorescence radiation by the three adjacent-slot flames in the field of view of the collection optics was of some concern. However, absorption measurements on the strongest transition through these flames did not reveal any noticeable attenuation of the beam.

2 Results

2.1 H_2CO *A-state lifetime measurements*

Excitation and fluorescence spectra were obtained in both flames from spatial locations below the visible blue flame cone. Figure 2a shows an excitation scan obtained for flame 1 in the region 339.0–339.3 nm of the $2^1_0 4^1_0$ vibronic combination band. When the excitation laser was fixed on the isolated line at 339.23 nm (asterisk in Fig. 2a) the dispersed fluorescence spectrum depicted in Fig. 2b was obtained (taken with a 0.5 m scanning monochromator) covering the wavelength region from 380 to 470 nm. The emissions from vibrational progressions in the excited state can be distinguished [26]. Excitation and fluorescence spectra provided unequivocal evidence for the presence of H_2CO in the flame.

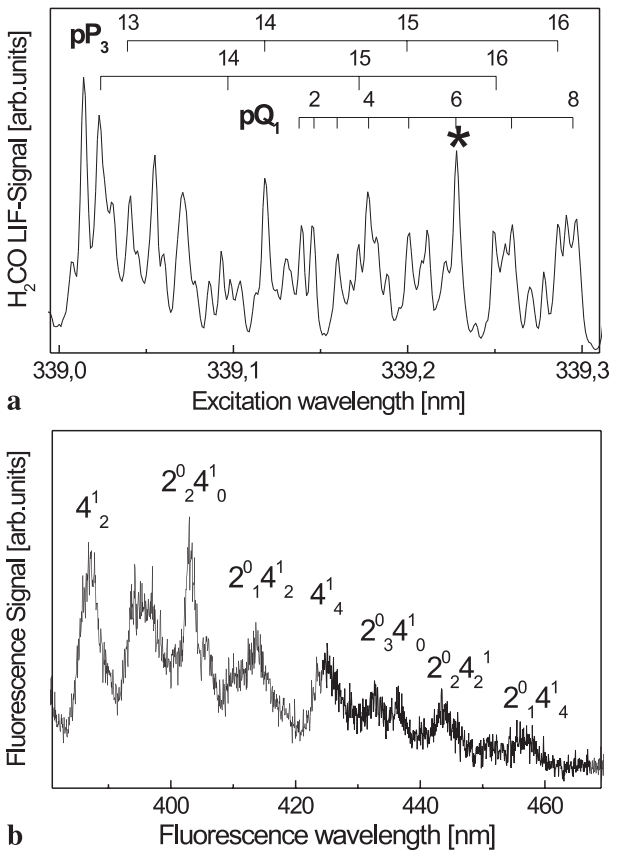

Fig. 2. a LIF excitation scan of the $2^1_0 4^1_0$ combination band of the H_2CO system at 339 nm recorded in flame 1. **b** Dispersed fluorescence spectrum of H_2CO after excitation of the $pQ_1(6)$ line in the $2^1_0 4^1_0$ combination band near 339 nm (marked "*" in **a**)

For the subsequent concentration and lifetime measurements we typically employed pulse energies of 100 μJ in the linear-excitation regime.

As outlined above, to account for the spatial variation of the collisional quenching environment in the measured formaldehyde LIF intensity, we directly determined the effective fluorescence lifetime as a function of height above the nozzle exit for each flame. A typical fluorescence-time profile after laser excitation is depicted in the inset of Fig. 3a (solid line) together with a Rayleigh signal (dashed line), obtained when the laser was tuned off resonance and the longwave-pass filter was removed, showing the temporal response characteristics of the present measurement setup. The obtained fluorescence traces were deconvoluted with respect to the temporal profile of the excitation laser, and effective lifetimes were derived from a biexponential fit to the resulting curves. In such a way the initial fast decay of the fluorescence signal intensity was properly taken into account. For all curves the fast decay time remained fixed around 5 ns probably reflecting some perturbation during the presence of the excitation pulse. As is shown in the main plot of Fig. 3a the

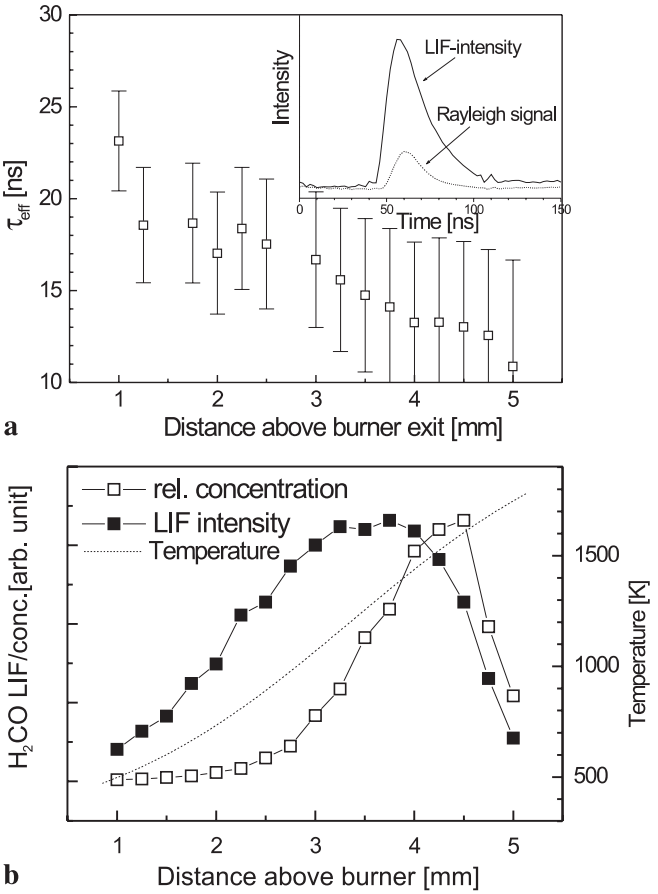

Fig. 3. a Effective fluorescence lifetime τ_{eff} of H_2CO after excitation of the $pQ_1(6)$ transition in the *A*-state as a function of height above the central slot for flame 1. The error bars denote a 2 times standard deviation from several fits. The *inset* shows a temporally resolved signal profile with the laser tuned on *(solid line)* and off *(dashed line)* the resonance line, respectively. **b** Height profile of the LIF signal intensity along the centerline of the central slot *(solid squares)*, and after correction for the measured variation in the fluorescence lifetimes *(open squares)* for flame 1. The temperature profile (*dotted line*, interpolated values) as obtained from CARS- and FWTC-measurements in the same flame [21] is also shown

evaluated (slower) effective lifetimes τ_{eff} in flame 1 gradually decrease from $(23 \pm 5\,\text{ns})$ close to the slot exit down to 11 ns towards the flame tip (located approximately at a height of 6.5 mm). It has to be mentioned that in a preliminary data evaluation, effective lifetimes were obtained that were approximately a factor of 1.5 larger than determined here [22], mostly because the biexponential fitting procedure was not employed. Based on these data, relative quenching corrections were made to the measured LIF intensity profiles using the following expression for the linear LIF intensity [27, 28]

$$S_1 = N f_B \frac{B}{c} E_L \frac{\Gamma_1}{\Delta\nu} \frac{\tau_{\text{eff1}}}{\tau_0} \frac{g}{4\pi} \tag{1}$$

where f_B is the Boltzmann factor, B the Einstein absorption coefficient for the excited rotational transition, E_L is the laser energy, Γ_1 the line-shape overlap, $\Delta\nu$ the laser bandwidth, τ_0 the average natural fluorescence lifetime of all vibronic transitions of the excited A-state in the wavelength region 380–470 nm, and g a correction factor to account for the optical collection and transmission efficiency. In addition, to account for the temperature dependence of the probed ground-state population density (i.e., the effective number of excited species), the partition function $Q(T)$ was calculated from the HITRAN database [29] using interpolated temperature values from the FWTC measurements [21]. The resulting corrected H_2CO species profile is presented in Fig. 3b (open squares) together with the original data (filled squares) and the FWTC temperature values (dashed line). Corrections are most prominent in the preheating zone, where temperatures are in the range 800–1300 K. From calculations it was found that, especially in this temperature range, the corrections are caused mainly by the temperature dependence of the ground-state population density, which varies by a factor of 4, whereas a decrease of only 30% is noticed in the range 1300–1500 K. The plots demonstrate the importance of these corrections in extracting useful information from the relative H_2CO LIF intensity profiles in this flame.

2.2 Absolute calibration

To determine absolute H_2CO concentrations in the flame we recorded a calibration signal S_2 from a reference cell filled with 4 mbar formaldehyde vapor at room temperature. According to (1), dividing the respective LIF intensities measured in the flame and immediately afterwards in the reference cell, with all other parameters (excitation energy, PMT voltage, etc.) kept constant, gives the following relation:

$$\frac{S_1}{S_2} = \frac{N_1}{N_2} \frac{f_{B1}}{f_{B2}} \frac{\Gamma_1}{\Gamma_2} \frac{\tau_{\text{eff1}}}{\tau_{\text{eff2}}} \tag{2}$$

Indices 1 and 2 refer to the flame and cell measurement conditions, respectively. The unknown number density N_1 can then be derived if the Boltzmann factor, lineshape overlap and effective lifetime ratios are known or can be estimated. The different excitation efficiencies prevailing in the two measurements due to broadening processes (Doppler, collisions), were taken into account by the lineshape overlap factors Γ_i. Therefore, in Fig. 4 we compared the linewidths of an isolated rotational transition in the respective excitation spectra recorded in the flame at 0.1 MPa (lower panel) and in the cell

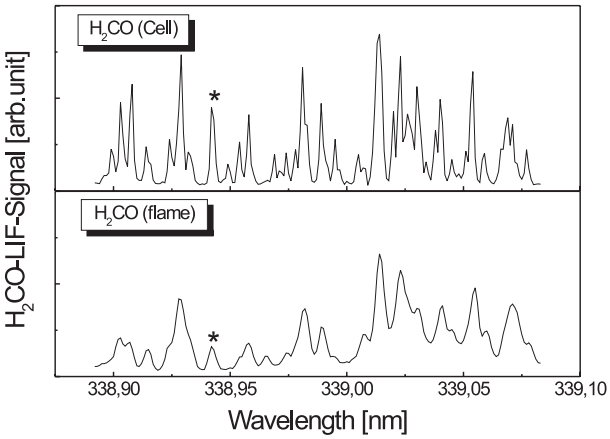

Fig. 4. LIF excitation spectra taken in flame 1 of the slot burner (*lower panel*) and in a reference cell at room temperature filled with 0.4-kPa (4 mbar) H_2CO vapor (*upper panel*). The "*" marks the transition used for the effective lifetime measurements (see text)

at 13.3 kPa (upper panel). The different lineshapes of the chosen transition (marked with an asterisk in Fig. 4) were fitted by Gaussian functions and their corresponding halfwidths accounted for in the Γ_i of (2). The respective τ_{eff} were again extracted by recording time-resolved fluorescence profiles in the flame and reference cell, respectively. This results in an effective fluorescence lifetime in the flame and cell environment of 17 and 123 ns, respectively. One advantage of this calibration method is that in (2) the unknown factors such as natural lifetime τ_0, absorption coefficient B and the detection efficiency g are canceled. Especially τ_0, which represents an average value of effective lifetimes from various vibronic states observed, would have been especially difficult to determine. Since the formaldehyde concentration (N_2) in the cell experiments is known and all other parameters denoted in (1) are equal, the absolute peak concentration of H_2CO in the flame finally was determined to be (174 ± 52) ppm in the fuel-rich flame 1 and (994 ± 298) ppm in the near-stoichiometric flame 2. The errors given are mostly due to temperature uncertainties.

3 Discussion

The absolute H_2CO concentration profiles are shown in Fig. 5 as a function of height for the rich (open squares) and lean (open circles) flames, respectively. Although a significant difference in the width of both profiles is obvious it can be recognized that formaldehyde is mainly formed at the beginning of the oxidation zone and before the steep rise in concentration of several radical species CH, NH and CN [22].

It is striking that the H_2CO absolute peak concentration level in the near-stoichiometric flame 2 ($\phi = 0.9$) is about 5 times larger than in the rich flame 1 ($\phi = 1.7$). The total amount of H_2CO produced in the lean flame (obtained by area-integrating the respective height profile in Fig. 5) exhibits a two-times-larger value than in the rich flame. Nevertheless, it is obvious that higher H_2CO concentrations were observed in the lean flame. This results from the fact that CH_4 oxidation in fuel-rich flames is dominated by the C_2 oxidation chain via recombination of methyl to ethane, rather than a C_1 pathway via methyl and formaldehyde [29].

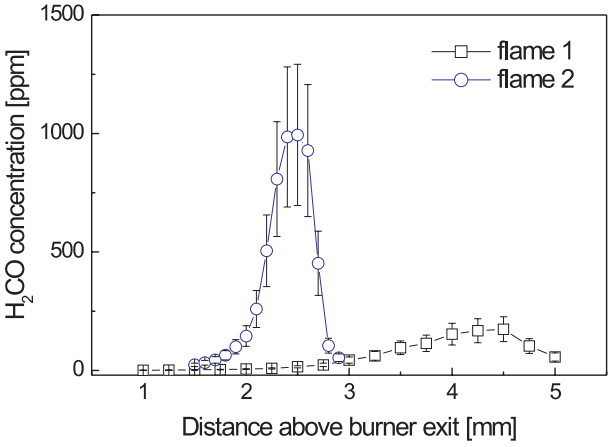

Fig. 5. Spatially resolved absolute H_2CO concentration profiles in flame 1 *(open squares)* and in flame 2 *(open circles)*, respectively, after quenching corrections and calibrations in a reference cell have been made

It is important to note the crucial role of the H_2CO fluorescence-lifetime measurements done here for the first time for local quenching corrections and to determine absolute concentrations. Comparisons of the present measurements with results from other work done in similar flames also exhibit concentration levels in the few-hundred-ppm range: Using probe measurements, Ashman et al. obtained H_2CO peak concentrations between 100–120 ppm in the preheating zone of a Bunsen burner [13]. Absorption measurements by Tolocka et al. [14] performed with a tunable diode laser spectrometer in a diffusion flame of a Wolfhardt–Parker burner gave a peak concentration of 400 ppm.

The absolute concentration profiles presented here represent, to our knowledge, the first quantitative investigation of nascent formaldehyde in flames via LIF. The calibration method introduced in this work can be extended to other species, provided lifetime measurements can be made with appropriate time resolution at atmospheric pressure and when other calibration techniques such as absorption are not sensitive enough. Together with spatial profiles of other species and temperatures in the same burner [21, 22], the present results constitute a valuable database for a stringent test of multidimensional flow simulations including full-chemistry models.

Acknowledgements. This work was supported by the European Community within the Brite Euram III program TOPDEC (Project BE 95 1523). D.I.S. acknowledges his DAAD fellowship as a graduate student at the University of Heidelberg. We thank Prof. B. Schramm for helpful discussions and for providing us with the formaldehyde samples.

References

1. J.A. Miller, C.T. Bowman: Prog. Ener. Combust. Sci. **15**, 287 (1989)
2. M. Frenklach, H. Wang, M. Goldenberg, G.P. Smith, D.M. Golden, C.T. Bowman, R.K. Hanson, W.C. Gardiner, V. Lissianski: Gas Research Institute Topical Report, Report No. GRI-95/0058, 1995
3. J. Warnatz, U. Maas, R.W. Dibble: *Combustion* (Springer, Berlin Heidelberg 1996)
4. J. Wolfrum: Hottel Lecture in Proc. Combust. Inst. **27**, 1 (1998)
5. C.B. Moore, J.C. Weisshaar: Ann. Rev. Phys. Chem. **34**, 525 (1983)
6. G.H. Dieke, G.B. Kistiakowsky: Phys. Rev. **45**, 4 (1934)
7. P.H. Paul, N.H. Najm: Proc. Combust. Inst. **27**, 43 (1998)
8. H.B. Najm, P.H. Paul, C.J. Mueller, P. Wyckoff: Combust. Flame **113**, 312 (1998)
9. J.E. Harrington, K.C. Smyth: Chem. Phys. Lett. **202**, 196 (1993)
10. N. Garland: Stanford Research Institute International Report MP 84–033 (1984)
11. B. Bäuerle, F. Hoffmann, F. Behrendt, J. Warnatz: Proc. Combust. Inst. **27**, 135 (1994)
12. R. Bombach, B. Käppeli: Appl. Phys. B **68**, 251 (1999)
13. P.J. Ashman, B.S. Haynes: Combust. Sci. Technol. **116**, 359 (1996)
14. M.P. Tolocka, J.H. Miller: Proc. Combust. Inst. **27**, 633 (1998)
15. J. Luque, D.-R. Crosley: Appl. Phys. B **63**, 91 (1996)
16. K. Kohse-Höinghaus, W. Perc, T. Just: Ber. Bunsenges. Phys. Chem. **87**, 1052 (1983)
17. W. Juchmann, H. Latzel, D.I. Shin, G. Peiter, T. Dreier, H.-R. Volpp, J. Wolfrum, R.P. Lindstedt, K.M. Leung: Proc. Combust. Inst. **27**, 469 (1998)
18. N.S. Bergano, P.A. Jaanimagi, M.M. Salour, J.H. Bechtel: Opt. Lett. **8**, 443 (1983)
19. R. Schwarzwald, P. Monkhouse, J. Wolfrum: Proc. Combust. Inst. **22**, 1413 (1988)
20. S. Yamagishi: *Proceeding Joint Meeting of the British, German and French Sections of the Combustion Institute*, Nancy, 1999, pp. 193–195
21. P.F. Miguel, N. Larass, M. Perrin, F. Lasagni, M. Beghi, S. Hasko, M. Fairweather, G. Hargrave, G. Sherwood, H. Levinsky, A.V. Mokhov, H. de Vries, J.P. Martin, J.C. Rolon, L. Brenez, P. Scouflaire, D.I. Shin, G. Peiter, T. Dreier, H.R. Volpp: *Proc. Intern. Gas Res. Conf.*, San Diego, Calif., 1998, pp. 461–472
22. D.I. Shin, G. Peiter, T. Dreier, H.R. Volpp. J. Wolfrum: Proc. Combust. Inst. 28, (2000) in press
23. R. Spence, W. Wild: J. Chem. Soc. 338 (1935)
24. J.D. Rogers: J. Phys. Chem. **94**, 4011 (1990)
25. H.N. Najm, O.M. Knio, P.H. Paul, P.S. Wyckoff: Combust. Sci. Technol. **140**, 369 (1998)
26. K. Shibuya, P.W. Fairchild, E.K.C. Lee: J. Chem. Phys. **75**, 3397 (1981)
27. J. Luque, D.R. Crosley: Appl. Phys. B **63**, 91 (1996)
28. J. Luque, W. Juchmann, J.B. Jeffries: Appl. Opt. **36**, 3261 (1997)
29. HITRAN database of infrared transition data, Air Force Geophysics Laboratory, 1996 edn.
30. J. Warnatz: In *Combustion Chemistry*, ed. by W.C. Gardiner, Jr. (Springer, New York 1984)